Research Article

Hacettepe University Journal of the Faculty of Pharmacy
Volume 45 / Number 2 / June 2025 / pp. 131-145

Cinnamomum verum: Biogenic Synthesis of Silver Nanoparticles and *In Vitro* Anticancer Activity on A-431 Cell Lines

Kusum JOSHI[1]
ORCID: 0009-0005-3792-3540
Sushma AWATI[2]
ORCID: 0009-0007-7864-9263
Anita DESAI[2]
ORCID: 0000-0003-1032-2604
Prabhu HALAKATTI[2]
ORCID: 0000-0003-2300-9692
Shantaveer IRAPPANAVAR[3]
ORCID: 0009-0004-4859-8870
Laxman VİJAPUR[2]*
ORCID: 0000-0003-2043-8862
Anil METRE[4]
ORCID: 0009-0003-5970-3747

[1] BVVS Hanagal Shri Kumareshwar College of Pharmacy, Research Scholar Department of Pharmaceutics, Bagalkot, Karnataka, India

[2] BVVS Hanagal Shri Kumareshwar College of Pharmacy, Department of Pharmaceutics, Bagalkot, Karnataka, India

[3] BVVS Hanagal Shri Kumareshwar College of Pharmacy, Department of Pharmacognosy, Bagalkot, Karnataka, India

[4] BLDEAS College of Pharmacy, Departmnet of Pharmaceutical Chemistry, Basavana bagewadi, Vijayapura, Karnataka, India

Corresponding author:
Laxman VİJAPUR
BVVS Hanagal Shri Kumareshwar College of Pharmacy,
Department of Pharmaceutics, Bagalkot, Karnataka, India.
E-mail: laxman906@yahoo.co.in
Tel: +919035608179

Received date : 23.01.2025
Accepted date : 27.05.2025

DOI: 10.52794/hujpharm.1625482

ABSTRACT

Human skin cancers are the most common type of cancer, especially among white individuals. Due to the rising incidence of cutaneous malignancies, various therapies have been developed. While surgical treatments remain the gold standard, innovative approaches are needed to reduce morbidity and mortality. This study explores the potential of green synthesized silver nanoparticles using *Cinnamomum verum* aqueous extract as an eco-friendly and cost effective alternative for skin cancer treatment. The plant extract served as a capping and reducing agent to biosynthesize silver ions into silver nanoparticles. Among the formulations, NP3 had the smallest particle size 220.5 nm and a zeta potential of -4.4 mV, as revealed by dynamic light scattering. Energy-dispersive X-ray analysis confirmed 26.18% silver content. The antiproliferative efficacy of NP3 was evaluated on A431 cell lines by cytotoxicity evaluation. The IC50 value for *Cinnamomum verum* extract was 57.92±0.25µg/ml, while biosynthesized NP3 had an improved IC50 of 45.30±0.72µg/ml, demonstrating significant antiproliferative activity. These findings suggest that biosynthesized silver nanoparticles could serve as an alternative therapy for managing skin cancer.

Keywords: Silver nanoparticles, *Cinnamomum verum,* A431cell lines, Skin cancer, MTT assay

1. Introduction

Nanotechnological applications for medical use have made the synthesis of nanoparticles with different shapes, sizes, and chemical compositions relevant. In the field of nanotechnology, a particle size is defined as a small entity that acts as a whole unit in respect to its transport and characteristics. Nanoparticles usually vary in size from 1 to 100 nm and possess distinct chemical and biological characteristics that differ greatly from those of bulk materials owing to their large surface relative to volume ratio and quantum effects. These properties make nanoparticles extremely useful in a variety of applications, especially in the field of healthcare. Ag-NPs stand out among metal-based nanoparticles due to their strong surface reactivity, simplicity of production, and versatility. Due to their distinctive catalytic, optical, and electrical capabilities, silver nanoparticles (Ag-NPs) have attracted a lot of attention. Due to their appealing physiochemical features, Ag-NPs frequently find applications in biology and medicine. Numerous pharmacological actions of Ag-NPs have been reported including antibacterial activity [1], antifungal activity [2], antiproliferativeactivity [3], antiviral activity [4], antiplasmodium activity [5] and mosquito larvicidal activity [6] etc.

Most of these chemically produced Ag-NPs are utilised for human purposes that pose serious risks to the environment and human health. Green synthesis of nanoparticles utilising microorganisms and plant extracts has gained popularity recently because it may be able to address the toxicity issue caused by chemical approaches.This environmentally friendly approach uses biological molecules as reducing and capping agents in the formation of nanoparticles. It prevents the use of toxic chemicals, reduces energy usage, and provides ecofriendly and stable nanoparticles.Green synthesis of silver metal nanoparticles using plant extracts have been studied previously using several plants which includes *Acalypha indica* [1], *Phyllanthus emblica* [7], *Panicum virgatum* [8], *Piper nigrum* [9], *Glycine max* [10], *Rosa rugosa* [11], *Camellia sinensis* [12]. These studies have shown that nanoparticles can be synthesized in environmentally friendly and green These studies have demonstrated that plant extracts can be used to create nanoparticles in an eco friendly and sustainable manner. The potential of traditional and medicinal plantsto create biocompatible nanoparticles is still being investigated in research on the green synthesis of Ag-NPs using extracts from these plants. Because every traditional plant has unique medicinal qualities, using these plants could improve the synthesized nanoparticles therapeutic qualities.The green synthesis of silver nanoparticles takes advantage of the intrinsic biological activity of medicinal plants, provides environmentally benign manufacturing, and yield nanoparticles with high biocompatibility and potential for a wide range of biomedical applications.

Cinnamonum verum, a member of the Lauraceae family, is one of the oldest plants used to season food. It has many traditional uses, including flavoring chewing gum, preventing bleeding, improving colon health, lowering the risk of colon cancer, promoting tissue regeneration, and acting as an antimicrobial, antifungal, antioxidant, antidiabetic, insecticidal, nematicidal, anti-inflammatory, anti-cancer, and mosquito larvicidal. Cinnamon has also long been used as a tooth powder and as a treatment for infections, bad breath, oral bacteria, and dental problems. Because of the significant phytochemicals found in the plant such as benzaldehyde, cuminaldehyd e,methoxycinnamaldehyde, hydrocinnamic aldehyde, benzenepropanal, citronellal, eugenol, pyrogallocatechin, gallic acid, terpins, and coumarinthe *cinnamonum verum* plant has been used for centuries [13-15].

The plant is a good option for biogenic synthesis of Ag-NPs because of the phytoconstituents listed above, which cap and convert silver to Ag-NPs. Phytochemicals present in *Cinnamon verum* act as both reducing and stabilizing agents during the synthesis of nanoparticles, Phytochemicals present in plant extract help convert silver ions (Ag^+) into nanoparticles (Ag^o), influencing their shape, size, and stability.This process may result in the production of environmentally benign and non-toxic green-synthesized Ag-NPs for biological and medical uses. Using an extract from *Cinnamonum verum* leaves, we will attempt to create nanoparticles in this work and assess their antiproliferative properties. This will give current people scientific support and possibly reveal the potential of *Cinnamonum verum* leaf Ag-NPs for their antiproliferative activity against A-431 cell lines.

2. Materıals and Methods

Cinnamomum verum leaves were collected and were authenticated by Prof. M.K.Ganachari, Department

of Botany, Basaveshwar Science College, Bagalkote (Ref No: BVVS/AW/2022-23/03 dated 04/02/2023). Silver nitrate of analytical grade was purchased from Loba Chemie Pvt LTD. Distilled water was used throughout the study.

2.1. Preparation of Cinnamomum verum leaf aqueous extracts (CVE)

The leaves were rinsed in distilled water three times. The cleaned leaves were left to air dry at room temperature in a shaded area as shown in Figure 1. The leaves were crushed when they had dried, and the powder was put away for later use. After soaking 10gms of crushed *Cinnamomum verum* leaves in 100 millilitres of distilled water for a full day, they were heated to 60 degrees Celsius for 15 minutes. A muslin cloth was used to filter the filtrate. After the extract has been run through Whatmann grade 1 filter sheets. The CVE was centrifuged at 5000 rpm for 15 minutes. The leaf extract was kept in a coloured amber glass jar at 4 °C for subsequent use [16-17].

2.2. Phytochemical screening of cinnamomum verum extract

The phytochemical screening for CVE was done according to the methods described by Khandelwal *et al*[18].

1. Test for Carbohydrates.

Molish test :2-3 ml of aqueous extract of CVE, add few drops of alpha-naphthol solution in alcohol shake and add Conc.$H_2SO_4$from sides of the test tube.

Fehling's test: Mix 1 ml Fehling's A & 1 ml Fehling's B solution with 2-3ml of CVE extract. Boil for one min add equal volume of test solution. Heat in boiling water bath for 5-10 mins.

Benedict's test: Mix equal volume of benedict's reagent and CVE extract in test tube heat in water bath 5 min.

2. Test for Monosachharides

Borfoed test : Mix equal volume of borfoed's reagent and CVEextract. Heat for 1-2 min in boiling water bath and cool.

3.Test for proteins :

Biuret test:To 3 ml of CVE extract add 4% NaOH& few drops of 1% cuso$_4$solution.

Millon'stest:Mix 3 ml of CVE extract with millon's reagent.

4. Test for glycosides

Test for cardiac glycosides

Baljet's test: Mix 3ml of CVE extract with Baljet reagentA section shows yellow to orange colour with sodium picrate

Legal's test: To CVE aqueous extract. Add 1 ml pyridine and 1ml sodium nitroprusside.

Liebrmann's Burchard reaction: Mix 2 ml of CVE extract with chloroform, add 1-2 ml acetic anhydride and 2 drops conc. $H_2SO_4$from the side of the test tube.

Liebermann test: Mix 3 ml of CVE extract with 3 ml acetic anhydride. Heat and cool add few drops of conc. H_2SO_4.

Test for saponin glycosides

Foam test: Shake the CVE extract vigorously with water. Persistent stable foam observed.

5. Test for tannins and phenolic compounds

To 2-3 ml of CVE extract add few drops following reagents.

a.5% Fecl$_3$ solution.

b.Lead acetate solution

c.Gelatin solution

d.Bromine water

e.Acetic acid solution

f.Potassium dichromate

g.Dilute iodine solution

h.Dilute HNO_3

6. Test forAlkaloids

Dragendorff's test : To 2-3 ml of CVE extract add few drops dragendorff's reagent.

Mayer's test: 2-3 ml of CVE extract with few drops mayer's reagent.

Hager's test: 2-3 ml of CVE extract with hager's reagent.

Wagner's test: 2-3 ml of CVE extract with few drops of wagner's reagent.

ISSN: 2458 - 8806

Tannic acid test: CVE extract is treated with tannic acid solution gives buff coloured ppt.

7.Test for flavonoids

Shinoda test: To CVE extract, add 5 ml 95% ethanol few drops conc. Hcl& 0.5 g magnesium turnings.

Sulphuric acid test: To CVE extract concentrated sulphuric acid was added.

8.Test for steroids

Liebrmann's Burchard reaction: Mix 2 ml of CVE extract with chloroform. add 1-2 ml acetic anhydride and 2 drops Conc. H_2SO_4 from the side of the test tube.

2.3. Biosynthesis of Ag-NPs

Silver nitrate and an aqueous extract of *Cinnamomum verum* (CVE) were utilized in the bioreduction of silver ions. Using 2 ml (NP1), 4 ml (NP2), and 6 ml (NP3) of varying concentrations of CVE, the Ag-NPs were biosynthesized. A 250 ml Erlenmeyer flask was filled with 1mM $AgNO_3$ to reach a volume of 100 ml. The flask was then left in a dark location for two hours. In the dark amber glass container, the colour changed from light yellow to yellowish-brown after two hours as shown in Figure 2. The CVE-Ag-NPs dispersion was centrifuged for 15 minutes at 10,000 RPM to produce the green synthesised CVE-Ag-NPs. After resuspending the nanoparticle dispersion in distilled water, it was centrifuged three times to remove any biological components that had not yet reacted. Ag-NPs were produced by using a hot air oven to dry the purified nanoparticle dispersion at 60°C. Characterisation studies were then conducted using these Ag-NPs [19].

2.4. Characterization of CVE-Ag-NPs

2.4.1. UV-Vis spectrophotometer analysis

The use of UV-visible spectroscopy was used to investigate the production of nanoparticles. SPR, which is produced by the resonant oscillation of conduction electrons at the interface of nanoparticles driven by incident light, is the most feasible technique for assessing the reduction of metal ions based on optical characteristics. With the use of a UV-Vis spectrophotometer, the biosynthesis of Ag-NPs was verified. Thus, in the UV–visible region, metallic nanoparticles have unique optical absorption spectra. Absorbance was measured between 200 and 800 nm. The solution of silver nitrate served as the blank. Using spectroscopy, the CVE-Ag-NPs dispersion was examined at room temperature [20].

2.4.2. Fourier Transmission Infrared spectroscopy (FTIR)

FTIR spectra of the dried biomass of CVE were obtained both prior to and following the silver nitrate bio-reduction procedure. The biomass was heated to 60˚C in order to dry the samples. The solid biomass of CVE/biosynthesized Ag-NPs was ground into an incredibly fine powder using potassium bromide (KBr). This powder was analysed after being compacted into a tiny pellet; KBr is transparent in the infrared. FTIR spectra were acquired by placing the pellet into the holder of the Fourier transform infrared (FTIR) spectrophotometer. The FTIR spectrum of the dried material was recorded [21].

2.4.3. Particle size and zeta potential measurement

The size of the nanoparticles and their zeta potential were measured using dynamic light scattering. To make the sample, ten millilitres of double-distilled water were used to dissolve one millilitre of CVE-Ag-NPs (NP1, NP2, and NP3) solution. The dispersion mixture was sonicated for 30 seconds in the sonicator to guarantee sufficient mixing. The sample was then placed inside a cuvette made of glass. Measurements were made when the laser light scattering was observed at a steady 90˚ angle [22].

2.4.5. Scanning Electron Microscopy (SEM) & EDAX

The synthesized CVE-Ag-NP micrograph images were captured using scanning electron microscopy. The process of creating sample thin films involved applying the sample sparingly on a copper grid covered with carbon, wiping away excess solution with blotting paper, and then letting the film on the SEM grid dry for five minutes under a mercury lamp before obtaining SEM images. 6 At 200 kV [23], Energy Dispersive X-ray (EDAX) examination was performed using a dry sample placed on a grid. Since EDAX analysis was performed for both qualitative and quantitative examination, it was possible to ascertain the kind of elements present and the proportion of each element's concentration within the CVE-Ag-NPs [24].

2.5. Antiproliferative activity of CVEVs Ag-NPs on A-431 cell lines

Trypsinization was followed by aspiration of the A-431 cells into a 15 ml centrifuge tube. The cell pellet came from centrifugation at 300 x g. To get approximately 10,000 cells in 200µl of suspension, the cell count was adjusted using Dulbecco's Modified Eagle Media (DMEM) medium. Each 96-well micro liter plate well received 200µl of the cell solution. At 37°C with 5% CO2 in the air, the plate was then incubated for 24 hours. Following a day, the used medium was aspirated. In the matching wells, 200µl of different concentrations of CVE/Ag-NP (20, 40, 60, 80, and 100 µg/ml from stock) were applied. The plate was then incubated in a 5% CO2 environment at 37°C for 48 hours. Following the plate's removal from the incubator, the media containing the CVE/AgNPs test sample was aspirated. To reach a final concentration of 0±5 mg/ml, 100µl of media containing 10% MTT reagent was added to each well. The plate was then incubated for three hours at 37°C in an environment with 5% CO2. Complete removal of the culture media was done without disturbing the crystals that had grown. The formazan was dissolved by gently shaking the plate in a ratory shaker after 100µl of DMSO solubilisation solution was added.The absorbance at 570 and 630 nm wavelengths was measured using a microplate reader. In order to determine the test drug concentration needed to inhibit cell growth by 50% (IC50), the percentage growth inhibition was calculated in triplicate after subtracting the background and the blank [25-26]. Further the IC_{50} values are seperate for CVE and NP3 difference in the mean was calculated using two tailed Z-test.

3. Results and Discussion

3.1. Phytochemical screening of Cinnamomum verum extract

On phytochemical screening *cinnamomum verum extract* was containing Carbohydrates, glycosides, Alkaloids, Flavonoids, Tannins and phenolic compounds

3.2. UV-Visible spectrophotometer analysis

Using UV-visible spectroscopy, the nucleation and production of CVE-Ag-NPs were observed, to confirm that Ag-NPs are nucleated. They used a UV-Vis

Figure 1. Leaves of *Cinnamomum verum*

Figure 2. Different concentrations of Ag-NPs

spectrophotometer. Since the UV-Vis spectrophotometer is the most practical instrument for monitoring the reduction of metallic ions, it was used to monitor the confirmation of Ag-NPs biosynthesis. Visual documentation of the CVE/silver nitrate combination's colour shift was made. After two hours, the dispersion colour turned dark due to Plasmon formation at the colloid surface, demonstrating that

ISSN: 2458 - 8806

Phytochemicals present in *Cinnamomum verum* extract

Test	Inference	Result
Test for carbohydrates		
Molisch's Test	Violet ring is formed at the junction of two liquids	Carbohydrates are present
Fehling's Test	First yellow then brick red ppt is appeared	Carbohydrates are present
Benedict's Test	Green color appeared	Carbohydrates are present
Test for monosacharides		
Test for Barfoed	Red PPT is observed	Carbohydrates are present
Test for glycosides		
Foam Test	Persistant stable foam observed	Glycosides are present
Test for flavonoids		
Test for shinoda	Orange to purple colour appears.	Flavonoids are present
Sulpuric acid test	Deep yellow solution appeared	Flavonoids are present
Lead acetate test	Yellow colour precipitate formed	Flavonoids are present
Sodium hydroxide test	Formation of colour	Flavonoids are present
Test for tannins and phenolic compounds		
5% FeCl3 Test	Deep blue-black colour appeared	Tannins and phenolic are present
Lead acetate test	White ppt	Tannins and phenolic are present
Bromine water	White ppt	Tannins and phenolic are present
Acetic acid solution	Decolouration of bromine water	Tannins and phenolic are present
Potassium dichromate	Red colour solution	Tannins and phenolic are present
Test for alkaloids		
Dragondorffs test	Orange Brown PPT is formed	Alkaloids are Present
Mayers Test	PPT is formed	Alkaloids are Present
Hagers Test	Yellow PPT is formed	Alkaloids are Present
Wagers Test	Reddish Brown PPT is formed	Alkaloids are Present
Tannic Acid	Buff coloured PPT formed	Alkaloids are Present

CVE-Ag-NPs were undergoing biosynthesis. The absorption spectra of the silver solution showed increasing intensity with time, as evidenced by the spectra taken before and after the addition of silver nitrate (two hours), suggesting that more CVE-Ag-NPs were forming in the dispersion. At the nanoparticle interface, incident light-stimulated resonant oscillations of conduction electrons form surface plasmon resonance (SPR). This leads to distinct optical absorption spectra for metallic nanoparticles.

Figure3a Displays the UV-Visible absorption spectra of CVE, while Figure3b displays the biosynthesised CVE-Ag-NPs.Because the strong band (SPR) was stimulated, the UV-visible spectra showed a notable band absorption peak at 420 nm Figure 3b indicating that the nanoparticles were isotopic and uniform in size. The absorption spectra of CVE-Ag-NPs were compared to that of silver nitrate. According to Mie's theory, spherical nanoparticles result in absorption spectra with a single surface Plasmon resonance band. The reaction mixture used in this study confirms single SPR bands, suggesting that CVE-Ag-NPs could have a spherical shape.

3.3. FT-IR analysis of Ag-NPs

Potential biomolecules involved in capping, effective stability, and reduction of silver nanoparticles are identified using Fourier transform infrared spectroscopy. Ag+ ion bio-reduction may have been aided by several phytoconstituents present in the CVE. Figure 4-5. presents the band strengths of CVE-Ag-NPs and plant extract in various spectrum regions that were examined. Fourier transform infrared spectroscopy, or FTIR, is used to identify possible biomolecules responsible for the reduction of Ag+ ions and the capping of the bioreduced silver nanoparticle produced by the leaf extract, as well as to ascertain the chemical composition of the CVE-Ag-NPs surface. The FT-IR spectra of the leaf extract and the CVE-Ag-NPs formulation are shown in Figure 4 and 5. Respectively. The N-H stretching vibration of amine compounds is recognised as the peak at 3266 cm^{-1} in the FTIR spectra of Ag-NPs mediated by *C. verum* leaf extracts. The symmetric and asymmetric C-H stretching of alkenes is responsible for the medium absorption peak of Ag-NP extract, which is situated at 2938 cm^{-1}. The peak in Ag-NPs at 1600 cm^{-1} is caused by the C=O bend of ketene. The peak at 1330 cm^{-1} is caused by the O-H bending of phenolic chemicals in plant extract. This implies that compounds such as alkaloids and tannins can be assumed. Ag-NPs are reduced and capped by the flavonoids saponin and cardiac glycosides included in the plant extract. The FTIR examination verifies the existence of organic groups such as phenolic and alcoholic [27].

3.4. Particle size and zeta potential measurement

The dynamic changes in light scattering intensity caused by the Brownian motion of the particles may be used to determine the size distribution of the particles. These observations yielded the average hydrodynamic diameter of the particles, the peak values of the hydrodynamic diameter distribution, and the width of the particle size distribution. NP1's CVE-Ag-NPs had a 446.0 nm particle size distribution and a 2.4 mv Zeta potential; NP2's saw a 382.0 nm particle size distribution and a 0.9 mv Zeta potential; and NP3's had a 220.5 nm particle size distribution and a -4.4 mv Zeta potential. Since NP3 had the largest surface area and the smallest particle size (220 ± 5 nm), it was chosen for further biological analysis and characterisation. Furthermore, NP3 could have strong antiproliferativeeffects on A-431 cell lines [28].

3.5. Scanning Electron Microscopy & EDAX

The size and form of the resultant particles were ascertained using SEM. Aliquots of the NP3 biosynthesised CVE-Ag-NPs were sonicated and sprayed over a carbon-coated copper grid, which was then left to dry at room temperature. An SEM picture was taken. Because the SEM measures actual diameter[5] and the DLS measures hydrodynamic size, Compared to the DLS analysis, the SEM found that the size identified was smaller. The generated CVE-Ag-NPs were spherical and polydisperse in form, as shown by the SEM images in (Figure7). The most common imaging signal in SEM is secondary electrons, which are abundant because source electrons can generate many secondary electrons.The atomic number of the chemical elements in the sample directly affects the amount of backscattered electrons that are produced. This region appears brighter the higher the atomic number. SEM is a flexible method for CVE-Ag-NP morphological detection. ImageJ version 1.4.3.67 was used to further analyze the nanoparticles seen in the SEM images. The software clearly displays the particles that were analysed as shown in Figure 6 and Figure 7. Toverify the average particle size. Summing the numbers in the Prism graphpad program yielded an average particle size of about 1.6 nm. These capped organic materials give the green synthesized CVE-Ag-NPs additional stability by preventing Ag-NP aggregation.

The EDAX analysis exposed the pureness and comprehensive chemical profile of Ag-NPs, revealing that Ag metal was present alongside other chemical elements in a specific proportion, as represented by a percentage. Upon evaluation of the reduced Ag-NPs via EDAX analysis, a significant peak was de-

ISSN: 2458 - 8806

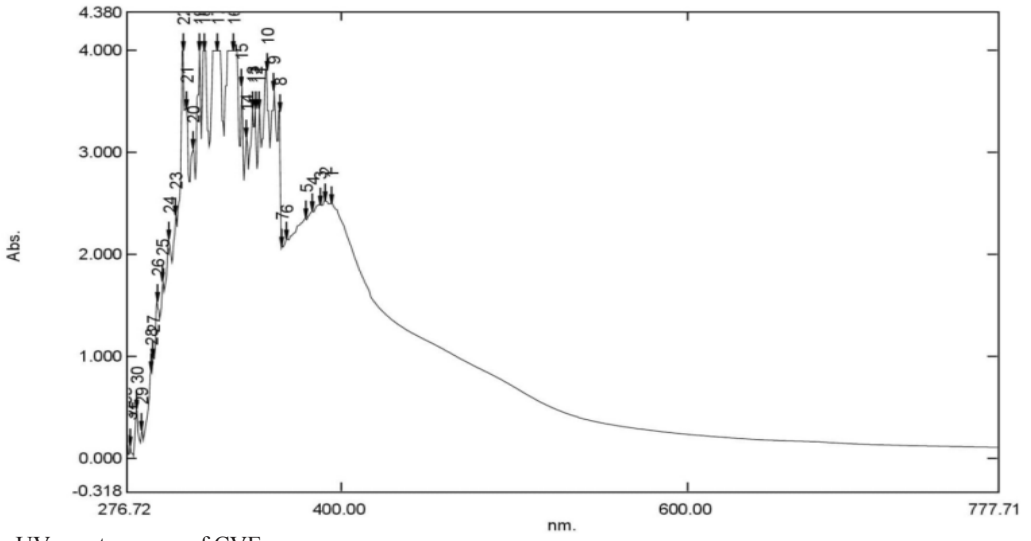

Figure 3a. UV-spectroscopy of CVE

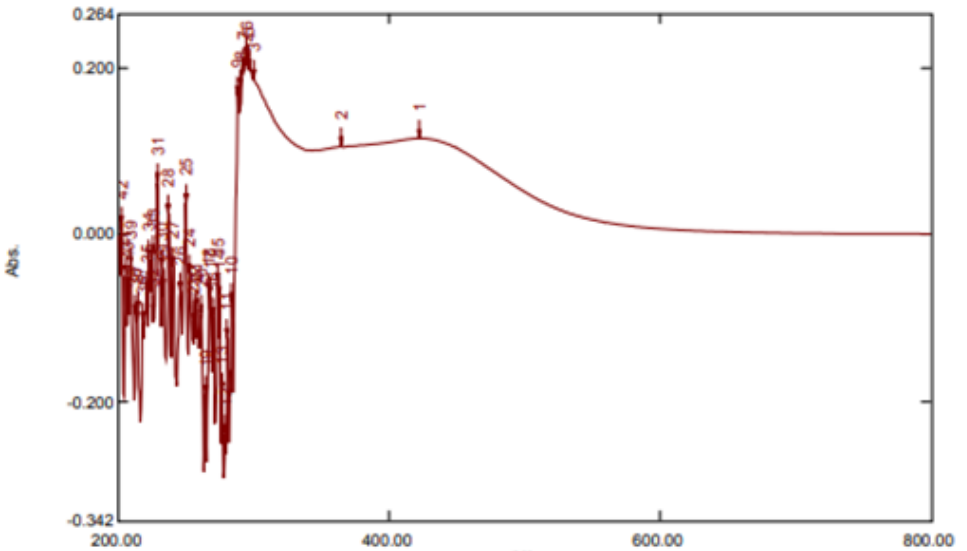

Figure 3b. UV-spectroscopy of biosynthesized Ag-NPs

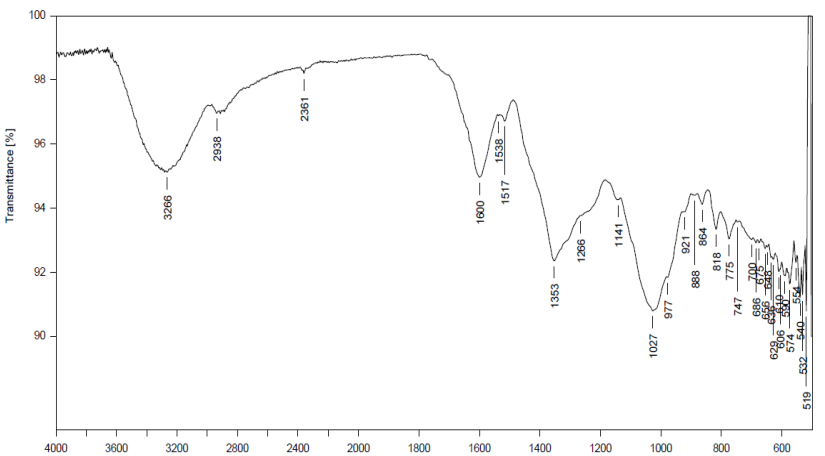

Figure 4. FTIR spectroscopy of CVE

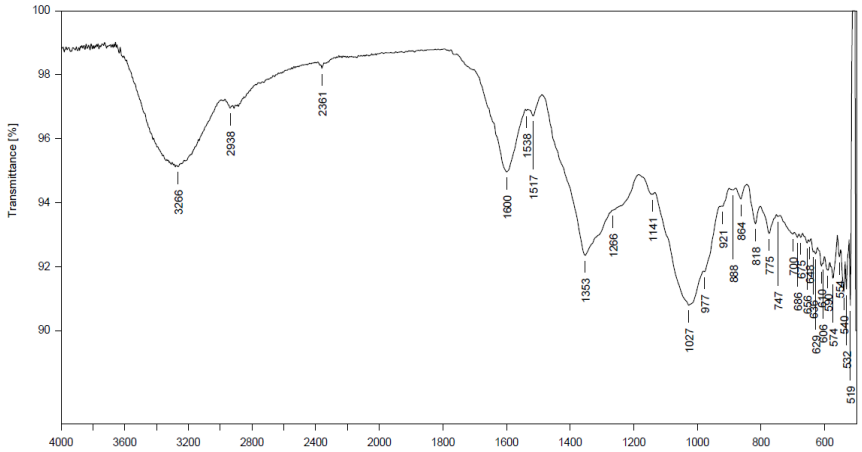

Figure 5. FTIR spectroscopy of biosynthesized nanoparticles

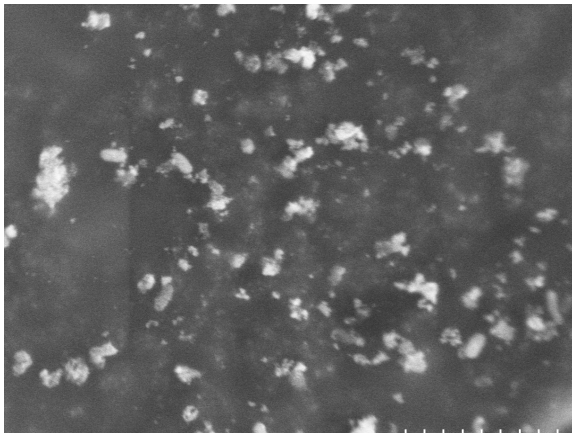

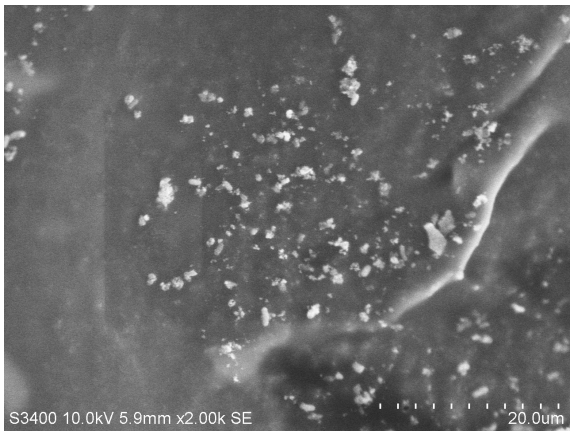

Figure 6. SEM of NP3

tected at 3keV. As shown in Figure 8 the EDAX examination demonstrated that silver (Ag) represented 26.18% of the overall composition and remaining 73.82% was phytoconstituents of CVE extract. Furthermore, both SAED and X-ray dispersive analysis provided credible evidence to support the presence of silver in the Ag-NPs [29].

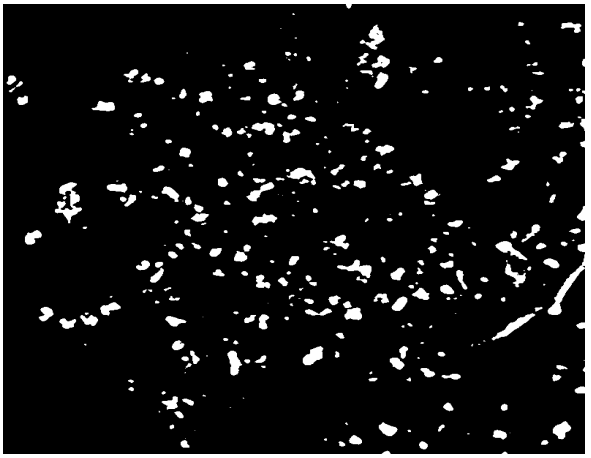

Figure 7. SEM image using J-image software

3.6. Antiproliferative activity of CVEVs CVE-Ag-NPs on A-431 cell lines by MTT assay

In recent years, tetrazolium salt reduction has become widely utilised to accurately measure cell proliferation. By reduction, the yellow tetrazolium MTT (3-(4, 5-dimethylthiazolyl-2)-2, 5-diphenyl tetrazolium bromide) is converted into reducing equivalents such as NADH and NADPH in metabolically active cells. This process is partially facilitated by dehydrogenase enzymes. One can use spectrophotometric methods to solubilize and quantify the intracellular purple formazan that results. By measuring the rate of cell proliferation, the assay also quantifies the decrease in cell viability that occurs when metabolic events result in apoptosis or necrosis. With rising incidence rates worldwide, the most dangerous and sometimes lethal kind of skin cancer is melanoma.

ISSN: 2458 - 8806

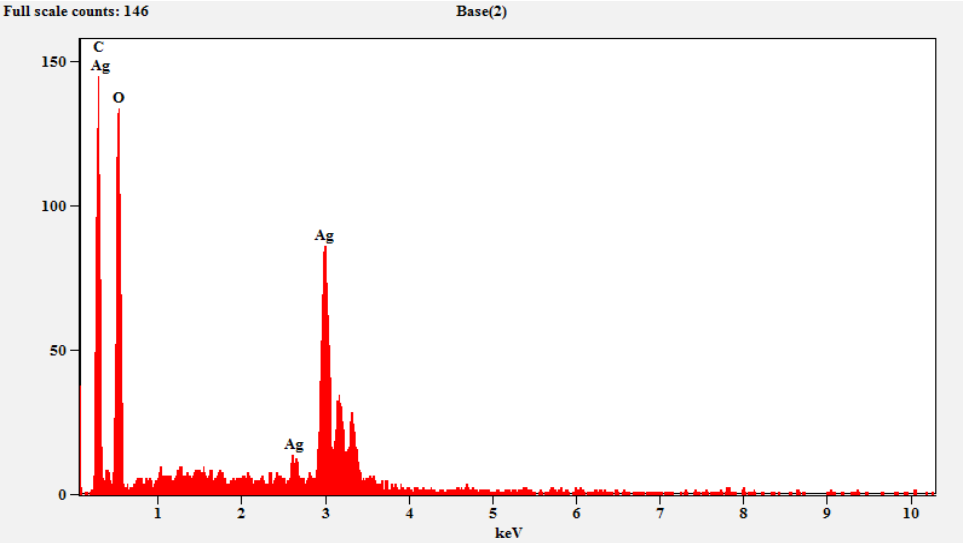

Figure 8. Energy dispersive X-ray (EDAX) analysis of NP3

Changes in the reproductive cycle and cell division processes associated with proliferative processes can affect the skin and result in different types of skin cancer.

These alterations result from the skin being exposed to a variety of outside elements, chiefly sunlight. Skin cancer development genes are mutagenized by UV radiation, which damages DNA. These genes exhibit the usual signature of UV-induced mutations, suggesting that UVB plays a role in the development of cutaneous carcinogenesis. In this study, the cytotoxicity of green synthesized Ag-NPs was investigated using the MTT test. NP3 was found to have anti-proliferative properties against human melanoma cell lines A431. It was found that at concentrations of 10µg/ml to 100µg/ml, increasing the concentration of CVE and Ag-NPs increased cell death, as shown in Figure 9-12. On the A431 Melanoma cancer cell line, the IC50 of CVE was 57.92±0.25µg/ml, whereas the IC50 of Ag-NPs that were biosynthesized was 45.30±0.72µg/ml. Z = 16.5 is very high, indicating a statistically significant difference between the two IC50 values. Z score of 16.5 corresponds to a $p < 0.001$, meaning the difference is highly significant.

The findings showed that human A431 melanoma cells were cytotoxic in a dose-dependent manner. Ajinkya et al., used the 5-Fluorocil to study the antiproliferative studies on A-431 cell lines and IC50 was 1.08µg/ml and for microemulsion IC50 was decreased to 0.79 µg/ml, indicating the greater penetration of the microemulsion to cells has greater antiproliferative property[30].At 100 µg/ml, CVE exhibited a cell viability rate of 17.62% while synthesized Ag-NPs (NP3) showed a viability rate of 14.42%. % Viability of A431 cell line compared to CVE and NP3 is displayed in (Figure10, 12). This could be because Ag-NPs at concentrations above 100µg/ml have a saturation effect on A431 cells. Ag-NPs that were biosynthesized caused more A431 cell death when compared to aqueous extract. Indeed, both AgNPs and *Cinnamomum verum* extract have independently demonstrated anticancer properties. However, in the current study, AgNPs were biosynthesized using *C. verum* extract, and therefore, the observed biological effect is a synergistic interaction between flavonoids, tannins, phenolic compounds and silver [31-32].

5-Fluorocil exhibits a lower IC_{50} than AgNPs, indicating a higher cytotoxic efficacy at lower concentrations against the A451cell line. 5-Fluorocil as a clinically optimized chemotherapeutic agent. As a pyrimidine analog, 5-Fluorocil acts as an antimetabolite that inhibits thymidylate synthase, an enzyme critical for DNA replication. Its mechanism of action is target-specific and cell cycle-dependent, primarily affecting rapidly proliferating cancer cells [33]. The lower IC50 observed reflects 5-Fluorocil's high affinity for its target and its optimized intracellular activation.

The biosynthesized AgNPs exhibited higher IC50 values, suggesting the requirement of higher con-

centrations to achieve comparable cytotoxic effects. This can be attributed to their broad-spectrum, non-specific mode of action, which includes generation of reactive oxygen species (ROS), disruption of mitochondrial membrane potential, and oxidative stress-induced apoptosis [34]. While effective, these mechanisms may require longer exposure times or greater doses to elicit maximal cytotoxicity. Furthermore, the cytotoxic efficacy of AgNPs is known to be influenced by factors such as particle size, shape, surface charge, and the nature of the capping agents used during green synthesis [35].

Another important consideration is the variability in cellular uptake mechanisms. While 5-Fluorocil enters cells via nucleoside transporters, ensuring efficient intracellular delivery, AgNPs depend on endocytosis, which may be less efficient and more variable between cell lines [36]. Moreover, the biosynthesized AgNPs in this study are capped with plant derived phytochemicals, which, although potentially bioactive, may introduce inconsistencies in particle behavior and stability.

Taken together, the observed difference in IC_{50} values reflects the contrast between a molecularly targeted chemotherapeutic agent and a broad-spectrum nanomaterial based cytotoxin. While AgNPs offer advantages such as multi-target action and reduced likelihood of drug resistance, 5-Fluorocil higher potency and predictability make it superior in scenarios requiring precise, high-efficacy treatment at lower doses.

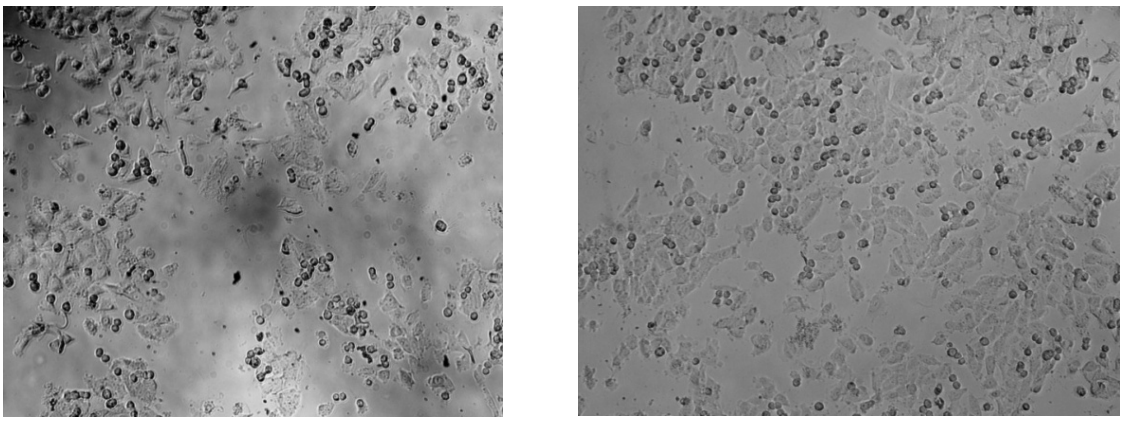

Figure 9. MTT assay microscopical images a) Untreated b) CVE

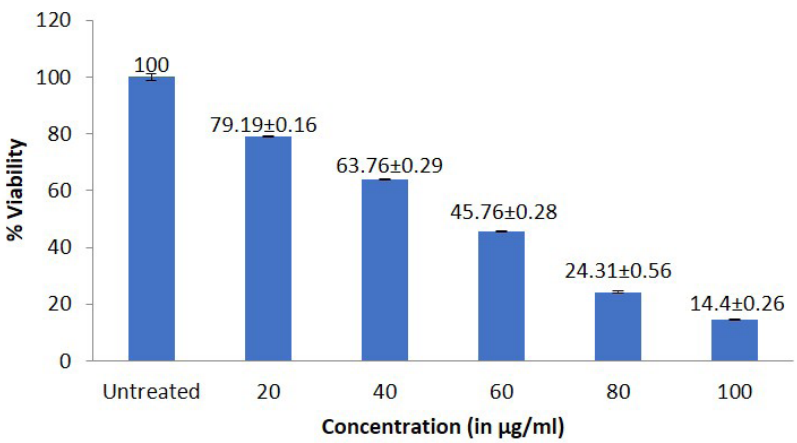

Figure 10. Percentage viability of A-431 cell line Vs NP3

ISSN: 2458 - 8806

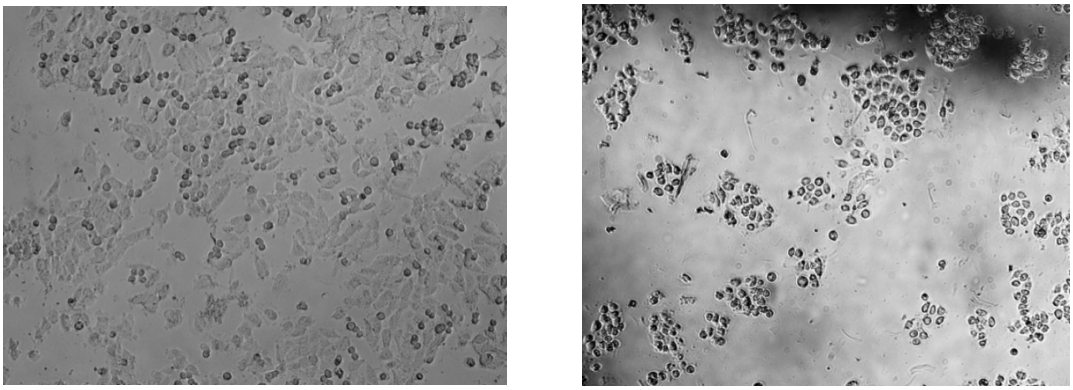

Figure 11. MTT assay microscopical images a) Untreated b) NP3

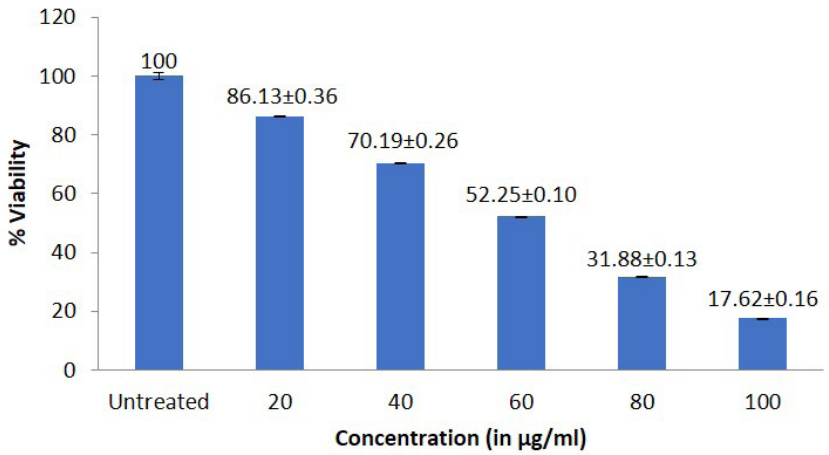

Figure 12. Percerntage Viability of A431 cell line Vs CVE

4. Conclusion

The current project was selected to create environmentally friendly Ag-NPs of CVE. The green synthesis approach used to biosynthesise CVEAg-NPs prevented product dangers that come with chemical and physical methods. From the study conducted the following conclusion were drown. *Cinnamomum verum* extract was prepared as 10% aqueous extract. The extract contained carbohydrates, saponins, alkaloids, flavonoids, tannins, and phenolic chemicals, according to a phytochemical analysis. CVE-Ag-NPs were prepared by using different concentration of aqueous extract with 1mM Silver nitrate. The UV-Vis spectrophotometer provided the initial proof of CVE-Ag-NPs production.The samples were scanned between 200 and 800 nm. Capping of silver was due to phytochemical of *Cinnamomum tamala* present in aqueous extract. Which result from the simultaneous vibration of metal nanoparticle electrons in resonance with light waves, creating a surface Plasmon resonance absorption band.. The surface Plasmon resonance spectrum for CVE-Ag-NPs was 420nm. Which is a typical absorption band for Ag-NPs. The IR spectra of the CVE and the biosynthesized Ag-NPs, showed a clear difference. Particularly the peak responsible for capping are Polyphenols, tannins, glycosides, flavonoids and alkaloids compounds. Thus, it was determined that the reduction of silver ions is caused by phenols, glycosides, flavonoids, and alkaloids. The particles were found to be polydispersed and primarily spherical in shape using scanning electron microscopy investigation. The EDAX analysis revealed that the silver was fabricated by *Cinnamomum verum* phytoconstituents. The synthesiz`ed extract of *Cinnamomum verum* Ag-NPs exhibited higher antiproliferativ eactivity. Both CVE and Ag-NPs showed an increase in antiproliferative activity that was dose dependent. Silver capping was caused by glycosides, alkaloids, and phenolic

chemicals, according to phytochemical analysis and infrared spectroscopy. The antiproliferative properties of *Cinnamomum verum* nanoparticles were improved as a result of the capping of phenols, tannins, saponins, and flavonoids. However, it is important to note that *in vitro* IC_{50} values do not fully capture therapeutic performance *in vivo*. The biosafety, pharmacokinetics, and systemic effects of AgNPs require further exploration before clinical applicability can be assessed. Future work should also investigate the potential of combination therapies using AgNPs and standard chemotherapeutics like 5-Fluorocil to explore possible synergistic effects.

Acknowledgements

This work was supported by Research grants for under Graduate students by Rajiv Gandhi University of Health Sciences, Bangalore Project Code: UG-22PHA446

Conflict of Interest

The authors declare no conflict of interest.

Statement of Contribution of Researchers

Concept-K.J.,L.V; Design– K.J.,L.V; Supervision-L.V; Resources – K.J; Materials – K.J.,L.V;S.A; Data Collection/or Processing – K.J., A.D; Analysis and /or Interpretation – K.J.,S.I; Literature search – K.J.,L.V; Writing- K.J., S.A., P.H; Critical Reviews-K.J.,S.A.,A.M.

References

1. Krishnaraj C, Jagan EG, Rajasekar S, Selvakumar P, Kalaichelvan PT, Mohan N. Synthesis of silver nanoparticles using Acalypha indica leaf extracts and its antibacterial activity against water borne pathogens. Colloids and Surfaces B: Biointerfaces. 2010;76(1):50–6. https://doi.org/10.1016/j.colsurfb.2009.10.008
2. Singh A, Jain D, Upadhyay MK, Khandelwal N, Verma HN. Green synthesis of silver nanoparticles using Argemone mexicana leaf extract and evaluation of their antimicrobial activities. Dig J Nanomater Bios. 2010;5(2):483-9.https://doi.org/10.1007/s13204-014-0366-6
3. Sriram MI, Kanth SBM, Kalishwaralal K, Gurunathan S. Antitumor activity of silver nanoparticles in Dalton's lymphoma ascites tumor model. Int J Nanomedicine. 2010;5:753–62. http://dx.doi.org/10.2147/IJN.S11727
4. Lu L, Sun RWY, Chen R, Hui CK, Ho CM, Luk JM, et al. Silver nanoparticles inhibit hepatitis B virus replication. Antiviral Ther. 2008;13(2):253-62. https://doi.org/10.1177/135965350801300210
5. Allahverdiyev AM, Abamor ES, Bagirova M, Ustundag CB, Kaya C, Kaya F, et al. Antileishmanial effect of silver nanoparticles and their enhanced antiparasitic activity under ultraviolet light. Int J Nanomedicine. 2011;3:2705-14.https://doi.org/10.1177/135965350801300210
6. Mondal NK, Chowdhury A, Dey U, Mukhopadhya P, Chatterjee S, Das K, et al. Green synthesis of silver nanoparticles and its application for mosquito control. Asian Pac J Trop Dis. 2014;4:S204–10. http://dx.doi.org/10.1016/s2222-1808(14)60440-0
7. Rosarin FS, Arulmozhi V, Nagarajan S, Mirunalini S. Antiproliferative effect of silver nanoparticles synthesized using amla on Hep2 cell line. Asian Pac J Trop Med. 2013;6(1):1–10. http://dx.doi.org/10.1016/S1995-7645(12)60193-X
8. Mason C, Vivekanandhan S, Misra M, Mohanty AK. Switchgrass (Panicum virgatum) Extract Mediated Green Synthesis of Silver Nanoparticles. World Journal of Nano Science and Engineering. 2012;02(02):47–52.http://dx.doi.org/10.4236/wjnse.2012.22008
9. Paulkumar K, Gnanajobitha G, Vanaja M, Rajeshkumar S, Malarkodi C, Pandian K, et al. Piper nigrum leaf and stem assisted green synthesis of silver nanoparticles and evaluation of its antibacterial activity against agricultural plant pathogens. Scientific World Journal. 2014;1:829894. http://dx.doi.org/10.1155/2014/829894
10. Vivekanandhan S, Misra M, Mohanty AK. Biological synthesis of silver nanoparticles using Glycine max (soybean) leaf extract: an investigation on different soybean varieties. J Nanosci Nanotechnol. 2009;9(12):6828–33 https://doi.org/10.1166/jnn.2009.2201
11. Dubey SP, Lahtinen M, Sillanpää M. Green synthesis and characterizations of silver and gold nanoparticles using leaf extract of Rosa rugosa. Colloids Surf A Physicochem Eng Asp . 2010;364(1–3):34–41. http://dx.doi.org/10.1016/j.colsurfa.2010.04.023
12. Vilchis-Nestor AR, Sánchez-Mendieta V, Camacho-López MA, Gómez-Espinosa RM, Camacho-López MA, Arenas-Alatorre JA. Solventless synthesis and optical properties of Au and Ag nanoparticles using Camellia sinensis extract. Mater Lett . 2008;62(17–18):3103–5. http://dx.doi.org/10.1016/j.matlet.2008.01.138
13. Simões MCF, Sousa JJS, Pais AACC. Skin cancer and new treatment perspectives: a review. Cancer Lett 2015;357(1):8–42. http://dx.doi.org/10.1016/j.canlet.2014.11.001

ISSN: 2458 - 8806

14. Singh N, Rao AS, Nandal A, Kumar S, Yadav SS, Ganaie SA, et al. Phytochemical and pharmacological review of Cinnamomum verum J. Presl-a versatile spice used in food and nutrition. Food Chem. 2021;338:127773. http://dx.doi.org/10.1016/j.foodchem.2020.127773

15. Narayanankutty A, Kunnath K, Alfarhan A, Rajagopal R, Ramesh V. Chemical composition of Cinnamomum verum leaf and flower essential oils and analysis of their antibacterial, insecticidal, and larvicidal properties. Molecules. 2021;26(20):6303. http://dx.doi.org/10.3390/molecules26206303

16. Vijapur LS, Hiremath JN, Bonageri NN, Desai AR. Murraya koenigii: biogenic synthesis of Ag-NPsand their cytotoxic effects against MDA-MB-231, human breast cancer cell lines. World J Pharm Med Res. 2019; 5:206-11

17. Vijapur LS, Srinivas Y, Desai AR, Gudigennavar AS, Shidramshettar SL, Yaragattimath P. Development of biosynthesized silver nanoparticles from Cinnamomum tamala for antioxidant, anti-microbial and anti-cancer activity. J. Res. Pharm. 2023;27(2):769-82http://dx.doi.org/10.29228/jrp.359

18. Khandelwal K. Practical Pharmacognosy.20th ed. Nirali prakashan: 2010 : 25.1-25.9.

19. Ahmed S, Ahmad M, Swami BL, Ikram S. Green synthesis of silver nanoparticles using Azadirachta indica aqueous leaf extract. J Radiat Res Appl Sci. 2016;9(1):1–7. https://doi.org/10.1016/j.jrras.2015.06.006

20. Jaast S, Grewal A. Green synthesis of silver nanoparticles, characterization and evaluation of their photocatalytic dye degradation activity. Current Research in Green and Sustainable Chemistry. 2021;4:100195.https://doi.org/10.1016/j.crgsc.2021.100195

21. Devaraj P, Kumari P, Aarti C, Renganathan A. Synthesis and characterization of silver nanoparticles using cannonball leaves and their cytotoxic activity against MCF-7 cell line. J Nanotechnol. 2013;1:1–5. http://dx.doi.org/10.1155/2013/598328

22. Elamawi RM, Al-Harbi RE, Hendi AA. Biosynthesis and characterization of silver nanoparticles using Trichoderma longibrachiatum and their effect on phytopathogenic fungi. Egypt J Biol Pest Contr. 2018;28:1-11https://doi.org/10.1186/s41938-018-0028-1

23. Vijapur LS, Shalavadi M, Desai AR, Hiremath JN, Gudigennavar AS, Shidramshettar SL, et al.Wound healing potential of green synthesized silver nanoparticles of Glycyrrhiza glabra linn root extract: A preclinical study. Journal of Trace Elements and Minerals. 2025;11:100214.https://doi.org/10.1016/j.jtemin.2025.100214

24. Anandalakshmi K, Venugobal J, Ramasamy VJ. Characterization of silver nanoparticles by green synthesis method using Pedalium murex leaf extract and their antibacterial activity. Appl Nanosci. 2016;6:399-8.https://doi.org/10.1007/s13204-015-0449-z

25. Kumbar VM, Muddapur UM, Bhat KG, Shwetha HR, Kugaji MS, Peram MR, et al. Cancer stem cell traits in tumor spheres derived from primary laryngeal carcinoma cell lines. Contemp Clin Dent. 2021;12(3):247-54. https://doi.org/10.4103/ccd.ccd_252_20

26. Van Meerloo J, Kaspers GJ, Cloos J. Cell sensitivity assays: the MTT assay. Methods Mol Biol. 2011;731:237-45.https://doi.org/10.1007/978-1-61779-080-5_20

27. Kumbar VM, Muddapur UM, Bhat KG, Shwetha HR, Kugaji MS, Peram MR, et al. Effect of curcumin on growth, biofilm formation and virulence factor gene expression of Porphyromonas gingivalis. Odontology. 2021;109(1):18-28. https://doi.org/10.1007/s10266-020-00514-y

28. Eya'ane Meva F, Segnou ML, Okalla Ebongue C, Ntoumba AA, Belle Ebanda Kedi P, Deli V, et al. Spectroscopic synthetic optimizations monitoring of silver nanoparticles formation from Megaphrynium macrostachyum leaf extract. Rev Bras Farmacogn. 2016;26(5):640-6.https://doi.org/10.1016/j.bjp.2016.06.002

29. Vijayakumar M, Priya K, Nancy FT, Noorlidah A, Ahmed AB. Biosynthesis, characterisation and anti-bacterial effect of plant-mediated silver nanoparticles using Artemisia nilagirica. Ind Crops Prod . 2013;41:235-40.https://doi.org/10.1016/j.indcrop.2012.04.017

30. Nikam AN, Jacob A, Raychaudhuri R, Fernandes G, Pandey A, Rao V, et al. Topical micro-emulsion of 5-Fluorouracil by a twin screw processor-based novel continuous manufacturing process for the treatment of skin cancer: Preparation and in vitro and in vivo evaluations. Pharmaceutics. 2023;15(9). http://dx.doi.org/10.3390/pharmaceutics15092175

31. Castro-Aceituno V, Ahn S, Simu SY, Singh P, Mathiyalagan R, Lee HA, Yang DC. Anticancer activity of silver nanoparticles from Panax ginseng fresh leaves in human cancer cells. Biomed Pharmacother. 2016;84:158-65. https://doi.org/10.1016/j.biopha.2016.09.016

32. Kwon H-K, Hwang J-S, So J-S, Lee C-G, Sahoo A, Ryu J-H, et al. Cinnamon extract induces tumor cell death through inhibition of NFkappaB and AP1. BMC Cancer.2010;10(1):392. http://dx.doi.org/10.1186/1471-2407-10-392

33. Longley DB, Harkin DP, Johnston PG. 5-fluorouracil: mechanisms of action and clinical strategies. Nat Rev Cancer. 2003;3(5):330–8. http://dx.doi.org/10.1038/nrc1074

34. AshaRani PV, Low Kah Mun G, Hande MP, Valiyaveettil S. Cytotoxicity and genotoxicity of silver nanoparticles in human cells. ACS Nano. 2009;3(2):279–90. http://dx.doi.org/10.1021/nn800596w

35. Ahmed S, Ahmad M, Swami BL, Ikram S. A review on plants extract mediated synthesis of silver nanoparticles for antimicrobial applications: A green expertise. J Adv Res. 2016;7(1):17–28. http://dx.doi.org/10.1016/j.jare.2015.02.007

36. Kaya MM. Silver nanoparticles stimulate 5-Fluorouracil-induced colorectal cancer cells to kill through the upregulation TRPV1-mediated calcium signaling pathways. Cell Biol Int. 2024;48(5):712–25. http://dx.doi.org/10.1002/cbin.12141

ISSN: 2458 - 8806